

Numerical modeling of airflow over the Ahmed body

Yunlong Liu, Alfred Moser

Air and Climate Group, Swiss Federal Institute of Technology, ETH-Zentrum WET A1, CH-8092 Zurich, Switzerland, Tel: +41 1 6326915, Fax: +41 1 6321023

Email: liu@hbt.arch.ethz.ch, URL: <http://www.airflow.ethz.ch/>

ABSTRACT

Airflow over the Ahmed body is investigated by means of transient RANS turbulence models. The simulations have been performed using two different differencing schemes. The performances of several RANS turbulence models have been compared. It has been found that Durbin's $k-\epsilon-v^2$ model is more accurate than the other turbulence models for the wall-bounded cases with separation and reattachment. A wall function for $k-\epsilon-v^2$ model has been introduced to avoid the divergence when very fine mesh is employed for complex geometries. Numerical results agree well with the reported experiments.

1. INTRODUCTION

In order to investigate the behavior of newly developed turbulence models for complex geometry cases, a simplified car model, known as the Ahmed body, has been tested by Ahmed, et al^[1] in the early 1980s. The Ahmed body is made up of a round front part, a moveable slant plane placed in the rear of the body to study the separation phenomena at different angles, and a rectangular box, which connects the front part and the rear slant plane, as shown in Figure 1. All dimensions listed in figure 1 are in mm. Several researchers have worked on the experiments and numerical modeling of the flow over the Ahmed body. Ahmed studied the wake structure and drag of the Ahmed body^[2-3], Lienhart and his colleagues^[4] conducted the experiments for two rear slant angles (25°, 35°) at LSTM. The velocities and turbulence kinetic energies have been measured by LDA at several key locations. This paper will take the LSTM test results as the validation data. Craft^[5] compared the performance of linear and non-linear $k-\epsilon$ model with two different wall functions. Basara^[6] conducted the numerical modeling of this case by means of large eddy simulation (LES), Menter^[7] compared the

performance of the SST model and some other turbulence models.

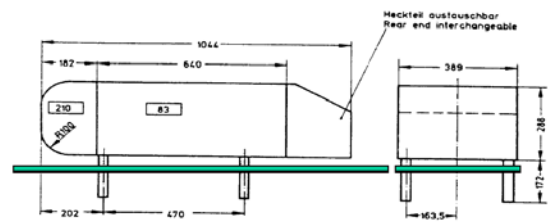


Figure 1: Schematic of the Ahmed body model^[1]

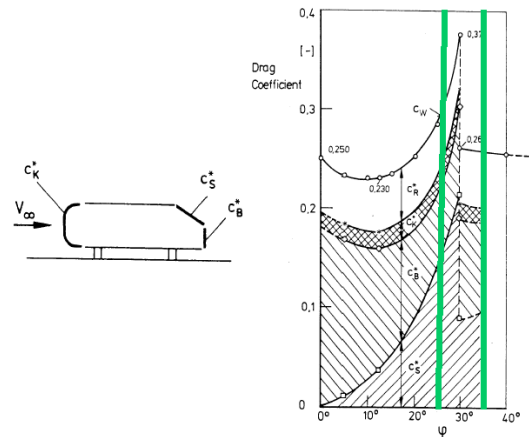


Figure 2: Characteristic drag coefficients for the Ahmed body for various rear slant angles ϕ measure by Ahmed^[1]

As the wake flow behind the Ahmed body is the main contributor to the drag force, accurate prediction of the separation process and the wake flow are the key to the successful modeling of this case. To simulate the wake flow accurately, resolving the near wall region using accurate turbulence model is highly desirable. This paper will study the effectiveness of three different turbulence models, including the $k-\epsilon-v^2$ model^[8-9],

the k-ε model and the full stress model, for the modeling of the flow over the Ahmed body, and shows the behavior of different turbulence models, as well as the effect of the grid layout and differencing schemes on the numerical results.

2. TURBULENCE MODELS

Airflow over the Ahmed body is governed by the Navier-Stokes equations. As turbulent flow is made up of a spectrum of vortex scales, the turbulence energy is distributed through the whole spectrum based on the wavelength. Ideally, resolving all the scales can offer the best insight into the understanding of the turbulent flow, which can be accomplished by direct numerical simulation (DNS). However, it is not practical to resolve all the scales for engineering problems such as the flow over the Ahmed body. While TRANS, a transient Reynolds averaged Navier-Stokes approach (RANS), offers a very promising approach because the large scales can be resolved while the small scales, which carry less turbulence energy compared to the large scales, are modeled by RANS sub-scale models. The averaged Navier-Stokes equations take the following form:

$$\frac{\partial \rho U_i}{\partial x_i} = 0 \quad (1)$$

$$\frac{DU_i}{Dt} = g_i - \frac{1}{\rho} \frac{\partial P}{\partial x_i} + \frac{\partial}{\partial x_j} \left[v \left(\frac{\partial U_i}{\partial x_j} + \frac{\partial U_j}{\partial x_i} \right) - \overline{u_i u_j} \right] \quad (2)$$

According to the Boussinesq assumption, the isotropic eddy viscosity/diffusivity formulation for Reynolds stress reads:

$$\overline{u_i u_j} = \frac{2}{3} k \delta_{ij} - v_t \left(\frac{\partial U_i}{\partial x_j} + \frac{\partial U_j}{\partial x_i} \right) \quad (3)$$

In the standard k-ε turbulence model, the Boussinesq assumption is applied together with wall functions. It is widely used and the convergence is stable. However, the above-mentioned assumption is not always true because of the an-isotropic nature of the flow in specific cases, such as the cases that involve the flows in the near wall region.

According to Launder^[10], the normal stress $\overline{v^2}$, perpendicular to the wall, plays the most important role to the eddy viscosity. Motivated by this idea, Durbin^[8-9] devised a three-equation model, known as the k-ε-v² model, or v2f model. The idea is to resolve the normal stress $\overline{v^2}$, along with solving the modified k and ε equations. The near wall region is resolved exactly and the wall-reflection is considered by means of elliptic relaxation in the model. It has

been reported^[8-9, 11-13] that this model is a significant improvement over the two-equation model for several test cases, such as channel flow, backward facing step, etc. Governing equations read:

$$\frac{Dk}{Dt} = P_k - \epsilon + \frac{\partial}{\partial x_j} \left[\left(v + \frac{v_t}{\sigma_k} \right) \frac{\partial k}{\partial x_j} \right] \quad (4)$$

$$\frac{D\epsilon}{Dt} = \frac{C_{\epsilon 1} P_k - C_{\epsilon 2} \epsilon}{T} + \frac{\partial}{\partial x_j} \left[\left(v + \frac{v_t}{\sigma_\epsilon} \right) \frac{\partial \epsilon}{\partial x_j} \right] \quad (5)$$

$$\frac{D\overline{v^2}}{Dt} = k f_{22} - \overline{v^2} \frac{\epsilon}{k} + \frac{\partial}{\partial x_j} \left[\left(v + \frac{v_t}{\sigma_k} \right) \frac{\partial \overline{v^2}}{\partial x_j} \right] \quad (6)$$

$$\frac{\partial}{\partial x_j} \left(\frac{\partial f_{22}}{\partial x_j} \right) - f_{22} = (1 - C_1) \frac{[2/3 - \overline{v^2}/k]}{T} - C_2 \frac{P_k}{k} \quad (7)$$

f_{22} is a quotient of the pressure strain Φ_{22} by the turbulent kinetic energy k

$$v_t = C_\mu \overline{v^2} T$$

$$C_\mu = 0.19, C_{\epsilon 1} = 1.44, C_{\epsilon 2} = 1.9,$$

$$\sigma_k = 1.0, \sigma_\epsilon = 1.3$$

$$P_k = v_t \left(\frac{\partial U_j}{\partial x_i} + \frac{\partial U_i}{\partial x_j} \right) \frac{\partial U_j}{\partial x_i}$$

The time scale T and length scale L can be obtained from the following:

$$T = \max \left\{ \frac{k}{\epsilon}, 6 \left(\frac{v}{\epsilon} \right)^{1/2} \right\}$$

$$L = 0.3 \max \left\{ \frac{k^{3/2}}{\epsilon}, C_\eta \left(\frac{v^3}{\epsilon} \right)^{1/4} \right\},$$

$$f_{22w} = - \frac{20v^2}{\epsilon_w} \left(\frac{v^2}{y^4} \right)_p, \text{ where index } w \text{ and } p$$

denote the values at the wall and that in the first cell above the wall, respectively.

To study the performance of the k-ε-v² turbulence model for application in complex geometries, several different turbulence models, including the k-ε model with wall function, the k-ε-v² model and full Reynolds stress model with wall function have been investigated in this paper. In this study, a wall

function for f_{22} is introduced in the near wall region for $k-\epsilon-v^2$ model.

Based on the numerical results for the channel flow DNS data of Kim^[14] et al (1987), in the near the wall region, we can get the non-dimensional value of f_{22} as a function of y^+ , so the f_{22} value for the first near wall cell can be obtained. The following formula is used to calculate the f_{22} value for the first near wall element:

$$f_{22}(y^+) = C_{\mu}^{0.5} k(0.65/(y^+ + 13.0) - 4.44/(y^+ + 13.0)^{1.58})/v \quad (y^+ \geq 20)$$

$$f_{22}(y^+) = C_{\mu}^{0.5} k[0.00199 + 2.511 \times 10^{-4}(y^+ - 20)]/v \quad (y^+ < 20)$$

It should be pointed out that the difference from Durbin's original model is that a value is given on the first point near the wall for f_{22} equation, along with the wall functions for the other equations, just like the case for the $k-\epsilon$ model. The purpose of this boundary condition for f_{22} equation is to improve the robustness of the original model.

3. PHYSICAL CASE AND NUMERICAL METHOD

The size of the computation domain is 7.044m long, 2.0m wide and 1.05m high, with the down stream portion extended five meters behind the rear of the Ahmed body. The Ahmed body is 1.044m long, 0.288m high and 0.389m wide, with a rear slant angle of 35° , as shown in figure 1. The projected area A_x of the Ahmed body in the mainstream direction is $0.112m^2$, which corresponds to a blockage ratio of 5.33%. The bottom surface of the Ahmed body is located at 0.05m above the ground. The incoming flow, located at one meter upstream of the front surface, is at 40 m/s with 0.2% free stream turbulence level, the corresponding Mach number is about 0.115, which gives a vehicle height based Reynolds number of 7.68×10^5 . Airflow is assumed to be incompressible, heat transfer is not considered in this study. Outflow is assumed fully developed and the zero-gradient velocity boundary condition is imposed. The ground and the body surfaces are treated as no-slip smooth walls. All the other boundaries are symmetry, because the size of the wind tunnel is much larger than the computation domain. Figure 3 shows part of the grid distribution near the Ahmed body symmetrical plane. Because of the complexity of this Ahmed body model, the computation domain has been split into 46 blocks, so that each processor is responsible for the

computation of several blocks. 16 processors are employed for parallel computation. To limit the total number of element cells, a non-uniform structured grid is constructed, with the near wall region using smaller grid size to control the first y^+ at around 20 to 50. Total element number is 460,000.

It has been found that the grid quality is crucial for convergence, and smaller time step is required in the initial stage to ensure the computation not to diverge. The differencing scheme can affect the accuracy of the solution, in the initial stage, the upwind differencing scheme is employed in the initial computation stage because it is robust, but it is not as accurate as second order central difference scheme. At time=0.6s it is switched to the second order central difference scheme to get a good final solution.

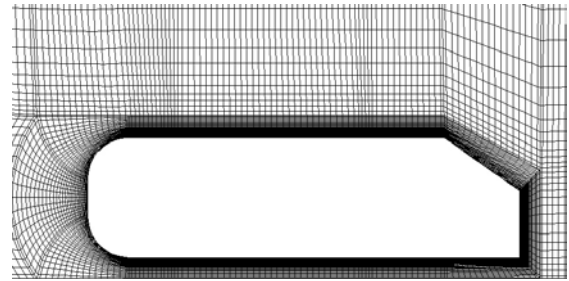


Figure 3: Grid distribution near the Ahmed body

4. RESULTS AND DISCUSSION

The results shown below are the averaged value over several cycles of the transient flow field, unless it is specially stated.

At upstream air velocity of 40m/s, an unsteady wake in the downstream is generated downstream. The unsteady wake comprises two vortices behind the rear with the larger one in the higher part, and the smaller one in the lower part, as shown in the streamline in figure 4. The background color in figure 4 shows the contour of the turbulent kinetic energy k . It is found that the peak value of k is located in the center of the small vortex downstream of the body, as observed in the experiment^[4].

Figure 5 shows the mean velocity and flow field in the symmetry plane of the Ahmed body. Vortical structures extend more than 0.5m beyond the end the body rear. The reverse flow climbs up to the rear slant, as observed in the experiment^[4].

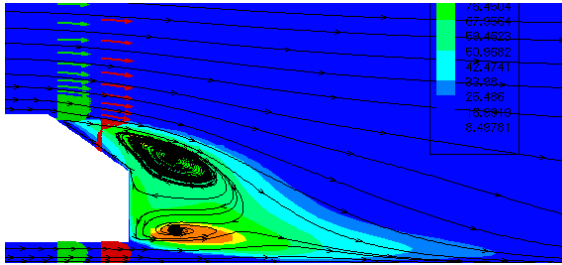


Figure 4: unsteady wake behind the body predicted using the $k-\epsilon-v^2$ model

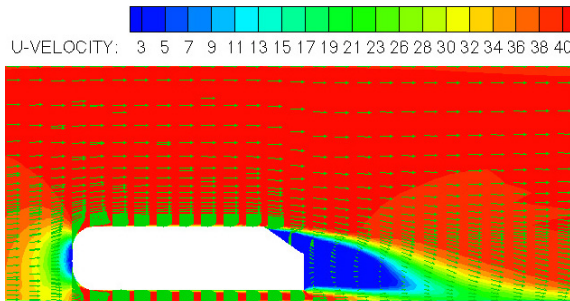


Figure 5: Flow field in the symmetry section colored by the stream-wise u-velocity predicted by the $k-\epsilon-v^2$ model

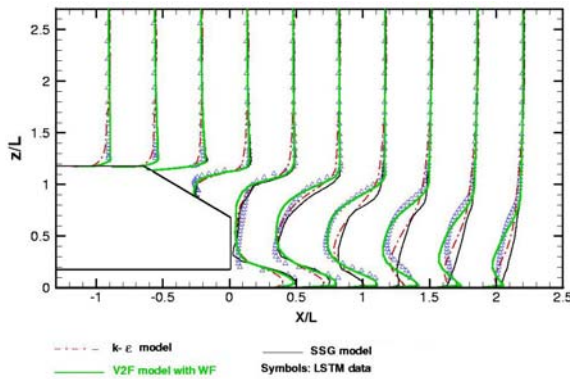


Figure 6: Comparison of velocity profile of numerical results and experiment

Figure 6 gives a mean velocity profile comparison of the numerical results with the experiments for the separation zone. Geometrical parameters are normalized by the height of the Ahmed body, L (0.288m). Compared with the standard $k-\epsilon$ model and full Reynolds stress model, the $k-\epsilon-v^2$ model gets better results for velocities above the rear slant and behind the Ahmed body, because the velocities predicted by the $k-\epsilon-v^2$ model fit well with the experimental data^[4]. The numerical results of the full stress model and the $k-\epsilon$ model predicted a wake being recovered too soon at the downstream, and predicted velocities have larger discrepancies when compared to the experiment data.

Figures 7a-d show the downstream development of the counter-rotating vortex system and contours of the predicted turbulent kinetic energy k at four different sections: 80mm, 200mm, 500mm and 1500mm downstream of the body, respectively. It confirms that two counter-rotating trailing vortices are generated downstream of the Ahmed body, and the vortices effect, though very small, still remains at more than 1.5m away from the rear, and the velocity deficit still visible at more than 4m behind the Ahmed body.

Figures 8 shows the drag coefficients predicted by the $k-\epsilon-v^2$ model. The time averaged drag force F_D is found by integration of surface pressure and the shear stress, the drag coefficient is defined as following:

$$C_D = \frac{F_D}{0.5\rho u_0^2 A_x}$$

Where ρ is the air density, u_0 is the upstream bulk velocity, A_x is the projected area of the Ahmed body in x direction.

It should be pointed out that before time=0.6s, the upwind differencing scheme is used. At time=0.6s, the differencing scheme is switched to the second order central differencing scheme. Its averaged value of the drag force coefficient is 0.262, which shows that the numerical result agrees quite well with the experiment data of Ahmed^[1], which is about 0.26, if the second order central differencing scheme is employed. This verified that, not only the turbulence model and the near wall grid resolution are affecting the accuracy of the predicted drag coefficient, the proper selection of the differencing scheme also plays an important role to make CFD more accurate.

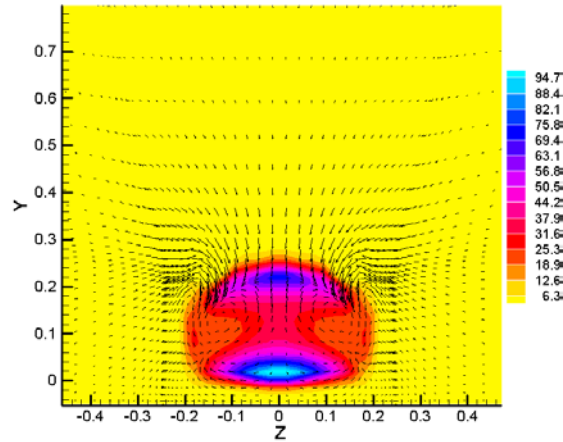
Table 1 gives a list of the measurement data and the predicted drag coefficient and its components, where C_k , C_B , C_S , C_D represents the drag coefficient at the nose, back, the rear slop and the total.

Pref is the reference pressure which is set to 0 Pa, when comparing the drag coefficients, the force components are sensitive to its location. In this paper the reference pressure is located at the outlet.

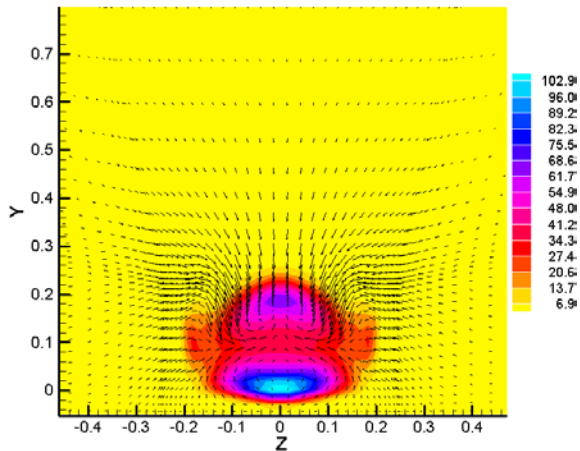
Table 1: Validation of drag force and force components

	C_k	C_B	C_S	C_D	Error%
Ahmed ^[1]	0.020	0.095	0.090	0.260	-
LSTM ^[4]	-	0.129	0.121	-	-
$k-\epsilon+WF$	0.026	0.105	0.111	0.242	-6.8
$k-\epsilon-v^2$	0.020	0.124	0.120	0.264	+1.5
SSG	0.010	0.102	0.098	0.210	-19.2
RSM	0.013	0.093	0.178	0.282	+8.5
SST	0.026	0.107	0.108	0.241	-7.3

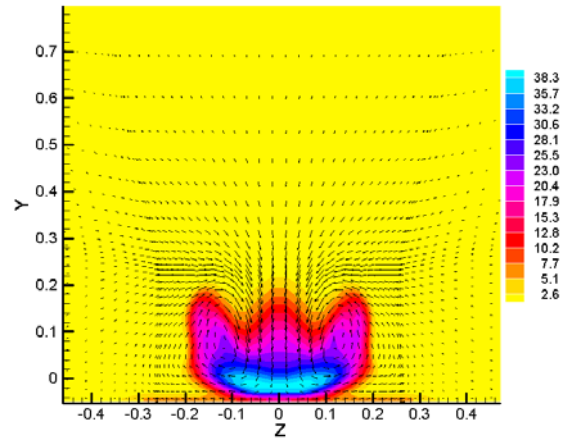
Based on the comparison of drag coefficients with LSTM experiment data, it can be concluded that Durbin's $k-\epsilon-v^2$ models gives the best result, followed by $k-\epsilon$, SST and RSM model.



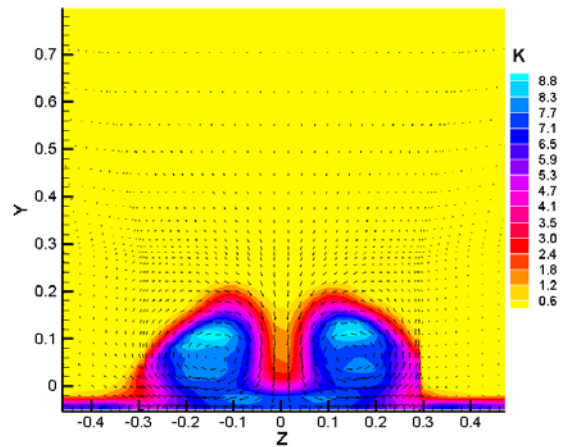
7a: 80mm



7b: 200mm



7c: 500mm



7d: 1500mm

Figure 7a-d: Velocities and contours of the predicted turbulent kinetic energy k at 80mm, 200mm, 500mm and 1500mm behind the body predicted by the $k-\epsilon-v^2$ model

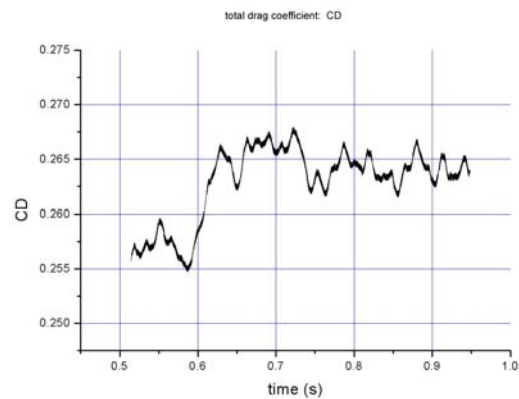


Figure 8: Drag force coefficient predicted by the $k-\epsilon-v^2$ model

5. CONCLUSIONS

The flow field and drag force of the flow over the Ahmed body can be simulated by computational approach. Compared with the standard k- ϵ model and the full stress model, the k- ϵ -v² model performs better, and the second-order central differencing scheme is more accurate than upwind scheme.

ACKNOWLEDGEMENTS

This study is supported by MOVA, a project undertaken by thermo-fluids section directed by professor K. Hanjalic. Part of this work is finished at TU Delft under the supervision of professor K. Hanjalic. Academic discussion with W. Khier, O. Ouhlous and M. Hadziabdic at TU Delft, The Netherlands, is gratefully acknowledged. Special thanks are extended to the Cray T3E computer center at Delft University of Technology, The Netherlands.

REFERENCES

[1] Ahmed, S.R., Ramm G.: Some Salient Features of the Time-Averaged Ground Vehicle Wake. SAE Technical Paper 840300, 1984.
[2] Ahmed, S.R., Wake Structure of typical automobile shapes. Transactions of the ASME, Journal of Fluids Engineering V103, P162-169, 1981
[3] Ahmed, S.R., Influence of base slant on the wake structure and drag of road vehicles. Transactions of the ASME, Journal of Fluids Engineering V105, P429-434, 1983
[4] Lienhart H., Stoots C., Becker S., Flow and turbulence structures on the wake of a simlified car model(Ahmed model), DGLR Fach. Symp. der AG ATAB, Stuttgart University, 2000.
[5] T. J. Craft, S. E. Gant, H. Iacovides, B.E. Launder, Computational study of flow around the Ahmed car body, 9th ERCOFTAC workshop on refined turbulence modeling, Darmstadt University of Technology, Germany, 2001
[6] B. Basara, Numerical simulation of turbulent wakes around a vehicle, *FEDSM 99-7324*, 1999
[7] L. Durand, M.Kuntz, F. Menter, Validation of CFX-5 for the Ahmed Car Body, 10th joint ERCOFTAC (SIG-15) -IAHR-QNET/CFD Workshop on Refined Turbulence Modelling, October 10-11, 2002
[8] Durbin P.A.: Near Wall turbulence closure modeling without “damping functions”. Theoretical and Computational Fluid Dynamics 3, P1-13, 1991

[9] Durbin P.A.: Separated Flow Computations with the k- ϵ -v² Model, AIAA Journal, V33, N4, PP659-664, 1995
[10] Launder, B. E., Low Reynolds Number Turbulence Near Walls, UMIST Mechanical Engineering Dept, Rept.TFD/86/4, University of Manchester, England, UK, 1986.
[11] M. Behnia, S. Parneix and P. A. Durbin, Prediction of heat transfer in an axisymmetric turbulent jet impinging on a flat plate. International journal of heat and mass transfer, V41, N12, PP1845-1855, 1998
[12] Georgi Kalitzin, Towards a robust and efficient v2f implementation with application to transonic bump flow, CTR Annual Research Briefs, PP291-299, 2000
[13] Lien F S, Durbin, P.A., Non-linear k- ϵ -v² modeling with application to high lift. Proc. of the summer program, CTR, NASA Ames/Stanford Univ. 5-22, 1996
[14] Robert D. Moser, John Kim and Nagi N. Mansour, DNS of turbulent channel flow up to $Re_{\tau}=590$, Physics of Fluids, V111, N4, PP943-945, 1999